

Surface Waves and Bottom Shear Stresses in the Yellow Sea

See Whan Kang and Jei Kook Choi

Korea Ocean Research and Development Institute, P.O. Box 17, Yeong Dong, Seoul

黃海에서의 波浪과 海底剪斷應力

姜 始 桓 · 崔 齊 國

韓國科學技術院 海洋研究所

Abstract: The amplitudes and periods of wind-driven, surface gravity waves in the Yellow Sea, were calculated using the SMB hindcasting method. Bottom orbital velocities and bottom shear stresses were then calculated on the basis of linear wave theory and Kajiura's (1968) turbulent oscillating boundary layer analysis. These calculations were made for northwesterly and southwesterly winds with a steady speed of 40 knots. The numerical results show that the wide offshore areas along the western Korean Peninsula are persistently subjected to the strong wave action and bottom shear stresses produced by the prevailing winds.

要約: 黃海의 海上風에 依한 重力波의 波高와 週期를 SMB法을 使用하여 計算하였다. 그리고 黃海에서 優勢한 北西風과 南西風이 40knots에 달할때의 波浪活動에 依한 海底流速과 海底剪斷應力을 線形波浪理論과 Kajiura(1968)의 亂流振動境界層分析에 依해 求하였다. 計算結果를 보면 韓半島의 西海沿近海에서 가장 큰 海波와 剪斷應力의 分布를 보이며 이로 因하여 沿近海底面이 持續的인 影響을 받고 있음이 나타났다.

INTRODUCTION

The wave action in the Yellow Sea has a significant effect on coastal processes such as shore erosion and sediment transport along the western Korean Peninsula. In order to determine the transport of sediments in a sea, various quantities must be known or be determined. Of critical importance is the rate at which sediments are entrained from the bottom into the overlying water. This entrainment rate can be directly related to wave action.

The primary sources of suspended sediments in the Yellow Sea are river inflows and shore erosion while the primary sinks are the deoposition and ultimate consolidation of sediments in the permanent sedimentary bottom of the sea. The sediment transportation from the primary sources to ultimate sinks occurs by frequent cycles of resuspension, transport, and deposition. The

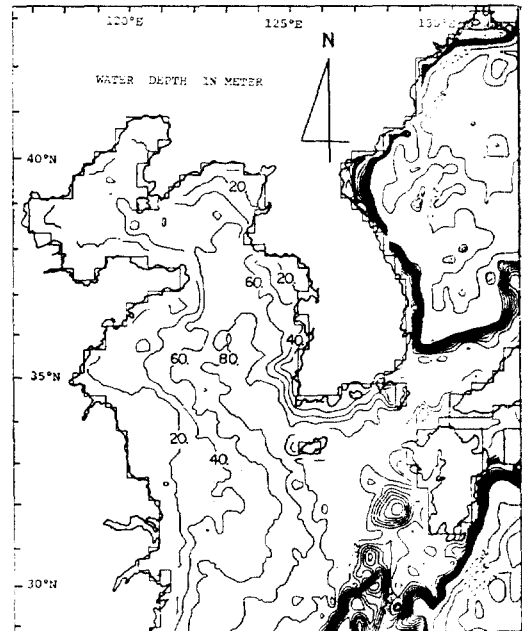


Fig. 1. Bathymetry of the Yellow Sea and adjacent seas of Korea. Numerical grids are shown along the coastal boundary.

resuspension occurs primarily due to wave action and currents, the former generally dominant in shallow water. The shallow Yellow Sea (Fig. 1) is significantly influenced by wave-sediment interaction, which leads to high sediment concentrations in the water. The wave-sediment interactions result mainly from strong wave action due to long fetches of prevailing winds.

MODEL EQUATIONS

Wave generation in shallow water is considerably modified by water depth and bottom surface conditions. In shallow water, wave heights are smaller and periods are shorter than in deep water. As the surface waves feel bottom, wave energy dissipation occurs due to bottom friction and percolation. For practical purposes, most of the wave prediction schemes for shallow water have been based on the SMB method (U. S. Army CERC 1977).

$$\begin{aligned} \frac{gH_s}{U^2} &= 0.283 \tanh \left[0.53 \left(\frac{gD}{U^2} \right)^{0.75} \right] \\ \tanh \left[\frac{0.0125 \left(\frac{gF}{U^2} \right)^{0.42}}{\tanh \left(0.53 \left(\frac{gD}{U^2} \right)^{0.75} \right)} \right] & \quad (1) \\ \frac{gT_s}{2\pi U} &= 1.2 \tanh \left[0.833 \left(\frac{gD}{U^2} \right)^{0.375} \right] \\ \tanh \left[\frac{0.077 \left(\frac{gF}{U^2} \right)^{0.25}}{\tanh \left(0.833 \left(\frac{gD}{U^2} \right)^{0.375} \right)} \right] & \quad (2) \end{aligned}$$

where H_s is the significant wave height, T_s the significant wave period, U the wind speed, F the fetch length, D the mean depth along the fetch, and g the gravitational acceleration. The significant wave height is the average height of the one-third highest waves in an observed wave train (say, containing approximately 100 waves), and is approximately equal to the average height observed by trained personnel. The significant wave period is the average period corresponding to the highest one-third waves. As the mean depth increases, equations (1) and

(2) reduce to the deep water relations.

For a progressive wave of small amplitude propagating in the x -direction in water of depth d , linear wave theory shows the following. The surface displacement η is given by $\eta(x, t) = a \cos(kx - \sigma t)$ where $k = 2\pi/L$ is the wave number, $\sigma = 2\pi/T$ the wave frequency, L the wave length, and T the wave period. The dispersion relation becomes

$$L = L_0 \tanh \frac{2\pi d}{L} \quad (3)$$

where $L_0 = gT^2/2\pi$ is the deep-water wave length and d the local depth. The maximum orbital velocity at bottom is given by

$$\bar{U} = \frac{\pi H}{T} \frac{1}{\sinh(2\pi d/L)} \quad (4)$$

The boundary layer flows under surface waves are oscillatory. In the presence of roughness elements on the bottom surface, the flow characteristics of the boundary layer are altered because of turbulent wakes and vortices. The surface conditions are either hydrodynamically smooth or rough, depending on whether the elements are completely submerged in the viscous sublayer or not. As shown in steady turbulent pipe flow (Rouse 1973), the transition criteria is $0.4 \leq h/D_i \leq 5$. Here, h is the particle size (say, *r.m.s.* roughness height), $D_i = 12\nu/U_m^*$ the thickness of the viscous sublayer, U_m^* the maximum frictional velocity, and ν the kinematic viscosity.

For an oscillatory boundary layer, the maximum shear stress exerted on the bottom sediments is given as

$$\tau_b = C_f \rho \bar{U}^2 \quad (5)$$

Here, ρ is the water density and C_f is a bottom friction coefficient which depends on both the surface roughness and the flow characteristics in the wave boundary layer. Kajiura (1968) proposed an expression for C_f based on the eddy viscosity assumption as follows. Over a smooth bottom, i.e., $h/D_i \leq 0.4$,

$$\frac{\kappa}{2C_f^{1/2}} + \ln \frac{1}{C_f^{1/2}} = \frac{\kappa N}{2} + \frac{\pi C_2}{2} - \gamma + \frac{1}{2} \ln \frac{\kappa}{N} + \ln R \quad (6)$$

where $\kappa=0.4$, $N=12$, $C_2=0.0593$, $\gamma=0.5722$, $R = \frac{U\delta^*}{\nu}$ the Reynolds number, and $\delta^* = (\nu/\sigma) +$ the wave displacement thickness. For $R < 200$, C_f is given approximately by

$$C_f = 1/R \quad (7)$$

Teleki and Anderson (1970) and Kamphuis (1975) showed that their laboratory shear-stress measurements agree with Kajiura's C_f over a smooth bottom. Over a rough bottom, i.e., $h/D_i > 0.4$,

$$\frac{\kappa}{C_f^{1/2}} + \ln \frac{1}{C_f^{1/2}} = \pi C_2 - 2\gamma + \ln \kappa + \ln \frac{\bar{U}}{\sigma Z_0} \quad (8)$$

Where $Z_0 = h/30$ is Nikuradse's equivalent sand roughness, $\frac{\bar{U}}{Z_0} = 30 R^2/R_h$, and $R_h = \frac{\bar{U}h}{\nu}$ the Reynolds number for roughness.

$$\text{For } \frac{\bar{U}}{\sigma Z_0} < 1000, C_f = 1.7 \left(\frac{\bar{U}}{\sigma Z_0} \right)^{-2/3} \quad (9)$$

The above relation for a rough bottom is generally acceptable compared to the published experimental data of Bagnold (1946), Jonsson (1966), and Yalin and Russell (1966). Figure 2 shows Kajiura's maximum C_f in an oscillating flow. C_f increases with decreasing Reynolds number R over a smooth bottom and with increasing roughness size over a rough bottom. In a natural ocean basin, the bottom surface conditions are highly variable. Also, small changes in bottom roughness may alter the vertical distribution of the eddy viscosity. Horikawa and Watanabe (1970) reported that the eddy viscosity attenuates with distance from the bed. Further research is needed to understand wave boundary phenomena for natural bottom conditions.

NUMERICAL CALCULATIONS

The Yellow Sea is approximately 1,000km

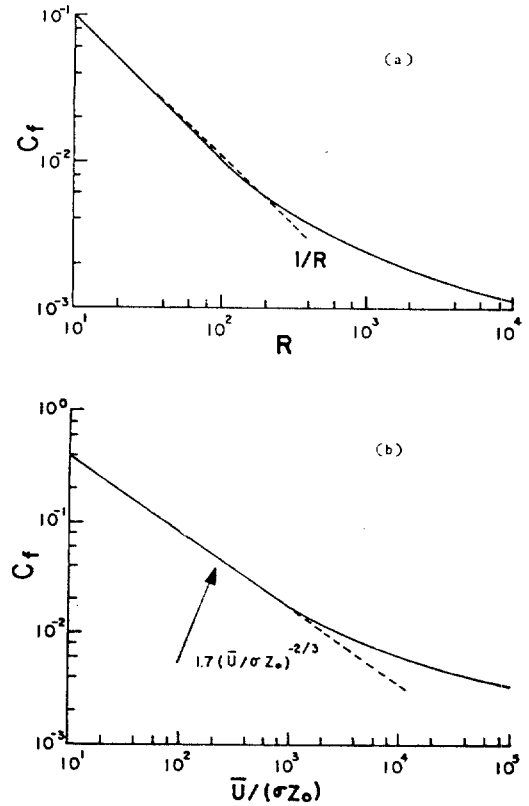


Fig. 2. Kajiura's frictional coefficients in an oscillating flow; (a) for a smooth bottom, (b) for a rough bottom.

long and 700km wide near the midpoint of its long axis, and is a relatively flat basin with an average depth of 40m (Fig. 1). The SMB method was employed to obtain surface wave information. A square horizontal grid with $\Delta x = \Delta y = 29\text{km}$ was used. At each grid point, the significant wave height and wave period were determined through equations (1) and (2) for given values of wind speed, fetch length, and mean water depth. The fetch length was defined as the distance in the direction of wind between grid point and shoreline. The mean depth was obtained by averaging water depths along the fetch. The wave length at each grid point was calculated by equation (3) using an iteration method. The wave number k and the ratio of d/L were determined. The maximum orbital velocity

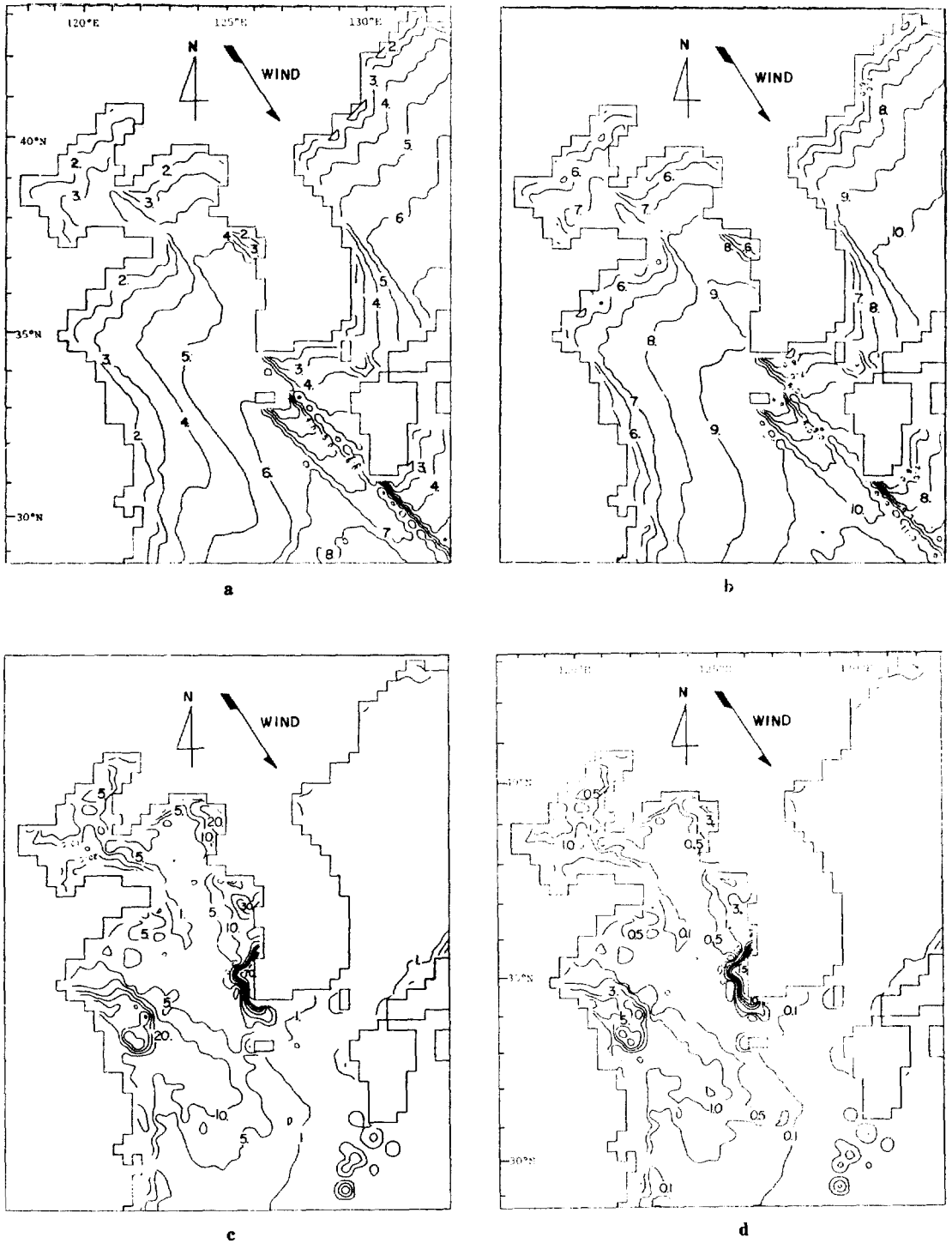


Fig. 3 a. Significant wave height (m) in the Yellow Sea for a northwesterly wind (315°, 40 knots). b. Significant wave period (sec) for a northwesterly wind. c. Bottom orbital velocity (cm/sec) for northwesterly wind. d. Bottom shear stress (dyne/cm²) for a northwesterly wind.

just outside the bottom boundary layer was calculated from equation (4) while the wave-induced bottom shear stress was from equation (5). Knowing bottom surface and flow conditions, the frictional coefficient C_f can be calculated using equations (6) to (9).

In the numerical calculations, a steady wind with a speed of 40 knots (approximately 20 m/sec) was assumed. This is a very strong wind for the Yellow Sea. Wind directions of northwest (315°) and southwest (225°) were assumed since they correspond to the two dominant wind directions (Meteorological Research Institute 1980). Because of the generally fine-grained and smooth bottom of the Yellow Sea, the bottom shear stress was calculated assuming a smooth wave boundary layer; thus the frictional coefficient C_f was determined through equations (6) to (7). Additional calculations were made and reported by Kang et al. (1984).

NUMERICAL RESULTS

Northwesterly Wind

The northwesterly wind is the most prevailing wind in the Yellow sea, during autumn and winter (Figs. 3a-d). The significant wave heights (Fig. 3a) range up to 5.5m while the wave periods (Fig. 3b) range up to 9 seconds. The ratio of water depth to wave length generally decreases with increasing fetch length. Transitional and shallow-water waves appear in most areas of the Yellow Sea Basin. The bottom orbital velocities (Fig. 3c) generally range 1 to 70 cm/sec. Along the west coast of Korean Peninsula, particularly in the middle and southern offshore area, the velocities are occasionally over 70 cm/sec. In the middle of the basin, the bottom shear stresses are in the range of 0.1 to 1 dyne/cm² (Fig. 3d).

Southwesterly Wind

Figures 4a through 4d show the results for the southwesterly wind which prevails in

summer. Wave heights (Fig. 4a) range up to 5.5m while wave periods are up to 9 seconds. Both wave height and period increase northeastward with increasing wind fetch. The larger waves can be seen in the nearshore regions of western Korean coast where the fetches are greater than in the other (China) side.

The bottom orbital velocities first decrease northeastward as the depth increases and then increase with decreasing depth (Fig. 4c) In the deeper parts of the basin (Fig. 1), the bottom orbital velocities become very weak (1 cm/sec) although the surface waves are large. The strong velocity distribution can be seen along the southwestern shore of Korea. In Fig. 4d, the bottom shear stresses follow the trend of velocity distribution. They are very strong in the near-shore regions of the Korean Peninsula.

DISCUSSION

Because of the shallow nature of the Yellow Sea, wave action is relatively strong and is important in redistributing the sediments from the rivers. For both the northwesterly and southwesterly winds, the wave action is always strongest in the coastal regions of the Korean peninsula.

Based on extensive textual analyses of Lake Erie sediments, Thomas et al. (1975) have shown that a mean grain-size distribution was very closely associated with an energy distribution, that is, hydraulic force exerted on the bottom surface. High energy zone consists of sand and gravel populations, representing nondepositional and erosional environments. Low-energy zone represents a depositional environment with dominant clay populations. The zone between them consist of mixed populations of sand and clay. As sediment mixing, resuspension, and transport are active, the surficial sediments are shown increasingly in a textual disequilibrium state.

In order to quantitatively relate the present

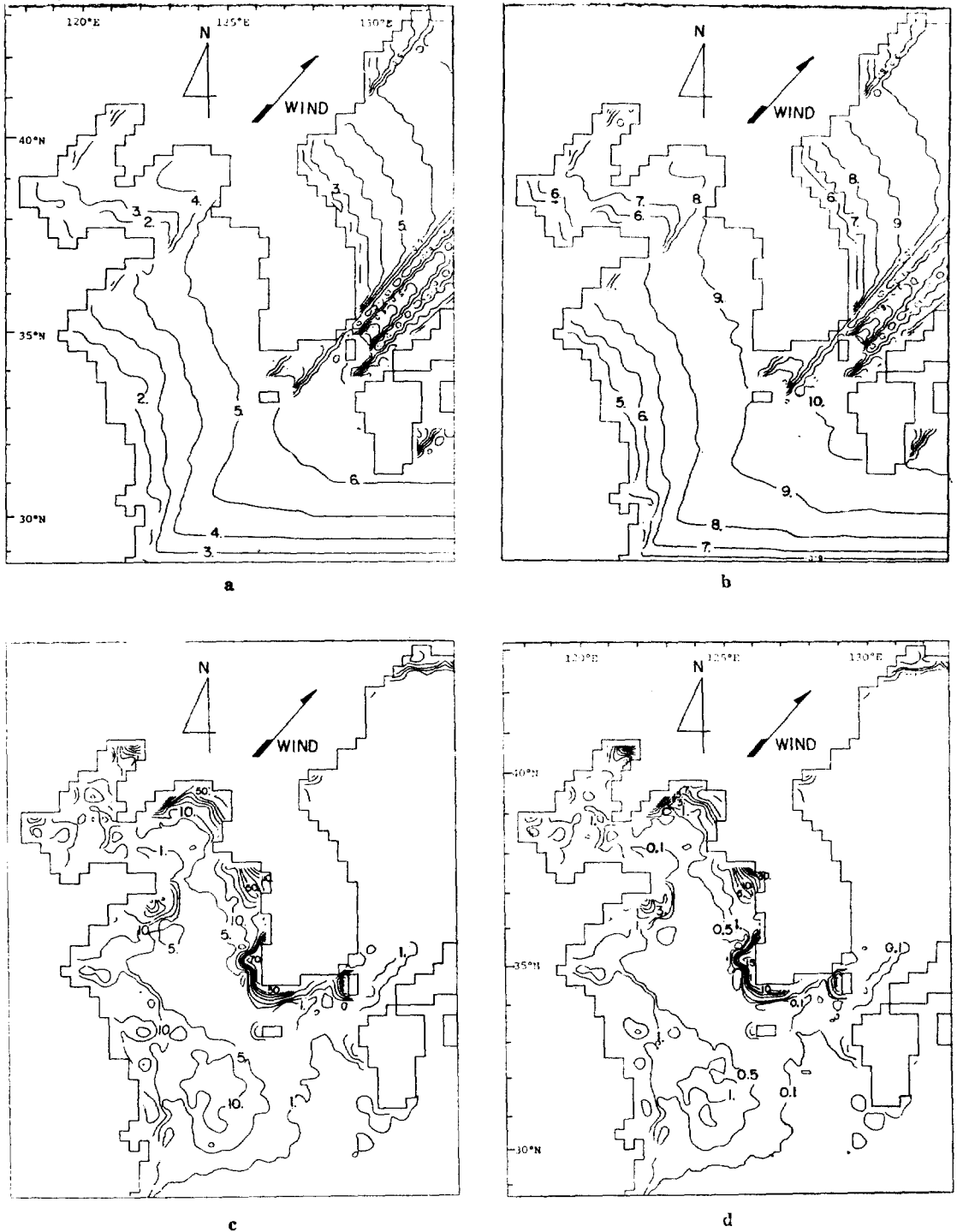


Fig. 4 a. Significant wave height (m) in the Yellow Sea for a southwesterly wind (225°, 40 knots).
 b. Significant wave period (sec) for a southwesterly wind. c. Bottom orbital velocity (cm/sec) for a southwesterly wind. d. Bottom shear stress (dyne/cm²) for southwesterly wind.